Lighting Models that Better Simulate Diffuse Reflection

Jose I.

June 14, 2022

1 Table of Contents

- Background
- Lambertian Reflection
- A Catalogue of Post-Lambertian Reflection Models
 - Lommel-Seeliger
 - Lunar Lambert
 - Minnaert
 - Hapke
- A Note on Other Models
- Bibliography

2 Background

Recently, I had taken an interest in reading about alternatives to the Lambertian reflection model in computer graphics. These include, but are not limited to the Hapke, Lommel-Seeliger, Lunar Lambert, and Minnaert models of diffuse reflection.

Perhaps a word is in order as to why I decided to pursue this track of "Alternatives to Lambertian Reflection." The Lambertian model is an idealization of diffuse scattering. However, the real world almost always features objects in which diffuse scattering is much more complex than that which can be approximated with the Lambertian model. Phenomena such as subsurface scattering, coherent backscattering, etc. are not accounted for; there exist more suitable models that can handle diffuse reflection more accurately. Other ways of handling reflection, such as adding in implementations of specular reflection or Snell's law to capture the behavior of dielectrics has also proven insufficient.

To discuss an example from historical science: one aspect of planetary photometry is the derivation of diffuse reflection models to accurately measure radiometric quantities of astronomical phenomena. For a long time, this meant the Moon, since in the night sky it is the brightest object. With the advent of telescopes that are able to image other objects in the Solar System, such models of the Moon's luminosity were tested against those other planets, asteroids, etc. Eventually some of these diffuse reflection models were discarded; others were refined based on the data. Thus, many of these models are said to be empirical (or semi-empirical), meaning that portions of them are based on experimental data, and not just theoretical calculations.

The aspect where computer graphics diverges from planetary photometry is that computer graphics uses radiometric quantities in a synthetic fashion, whereas planetary photometry uses them in an analytic fashion. For example, one goal in planetary astronomy is to use radiometric quantities to study some other aspect of the astronomical body's associated's properties: if you know the radiance of a satellite, you can partly answer the question "what does the planet's raidance tell you about the planet's atmosphere, geologic history, chemical composition?" In computer graphics, we are more interested in using these quantities to make objects that are visually consistent and thus interesting or "realistic" to the audience.

Thus, the aspects of the models from physical science that may be of interest to computer graphics researchers are those that accurately capture some visual phenomenon in a new way. For example, it's entirely possible that certain phenomena that affect our impression of stars and the Moon–such as atmospheric extinction and subsurface scattering—might be accurately captured by these diffuse reflection models.

3 Lambertian Reflection

Let us begin with the Lambertian treatment of diffuse reflection. The Lambertian model has two key properties: its intensity follows Lambert's cosine law, and the radiance is isotropic. The fact that its radiance is isometric means that we do not need to explicitly implement a phase function so that we perform importance sampling in some directions. Lambert's cosine law is often stated as:

$$I_O = L \cdot NI_I$$

where:

 I_O is the intensity of the outgoing beam, N is the normal vector of the surface struck by the beam I_I is the intensity of the incoming beam.

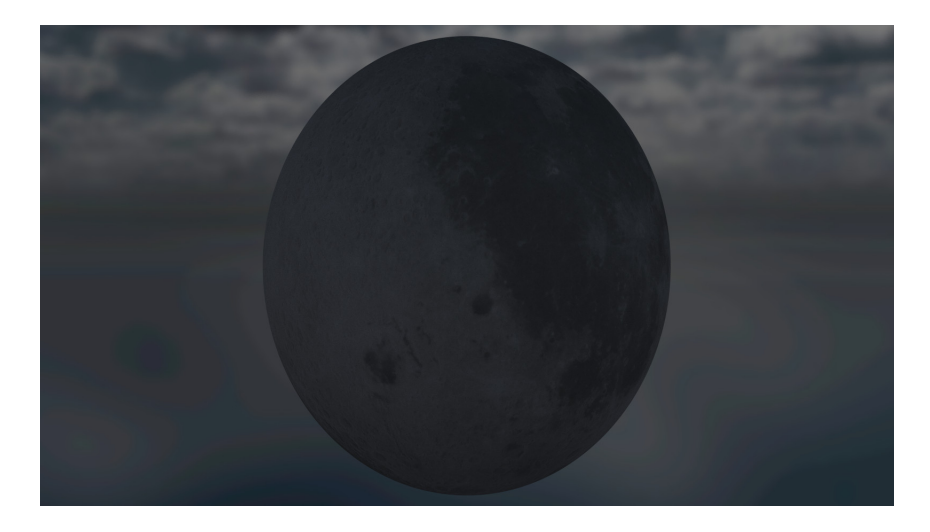


Figure 1: A figure of the Moon lit only using Lambertian Reflection

In our code, (which uses ray tracing to simulate how a scene looks,) the intensity of the outgoing beam is calculated by simply choosing a 3D vector from the unit sphere uniformly at random. The dot product is computed against the model's normal vector to calculate, and the value of the incoming beam is calculated from ray-trace recursion.

When we implement this, the following image of the Moon is produced. Note that the look is relatively "flat" as is consistent with isotropic scattering.

4 A Catalogue of Post-Lambertian Reflection Models

The previous treatment of Lambertian Reflection can be found easily on Wikipedia, and is treated in many standard computer graphics texts, such as in Peter Shirley's Ray Tracing in One Weekend series. The following extensions to Lambertian Reflection come from astronomical research. A textbook that covers aspects of planetary photometry should provide the details of these models; for our purposes, the text most cited will be Michael K. Shepard's Introduction to Planetary Photometry. The interested reader is advised to consult this or a similar text.

4.1 Lommel-Seeliger

In the 20th century, planetary astronomers were puzzled by the idea of opposition surge, or the brightening of an object when it is illuminated by the observer



Figure 2: The Moon lit using the Lommel-Seeliger model.

from behind. One structure that was affected by this phenomenon is Saturn's Rings. The Lommel-Seeliger model grew out of those attempts to capture this effect in mathematical form.

The Lommel-Seeliger model, like the Lambert model, assumes that scattering is isotropic. It also assumes that secondary scattering events are negligible; it only counts the photons that are scattered once. The full details of integrating over all possible scattering events at some optical depth is presented fully in the text Shepard; for our purposes we are interested only in the final BRDF:

$$r = \frac{w}{4\pi i} \cdot \frac{\mu_0}{\mu + \mu_0}$$

 $r = \frac{w}{4pi} \cdot \frac{\mu_0}{\mu + \mu_0}$ The following figure illustrates the result of illuminating the Moon using the Lommel-Seeliger model:

It has been pointed out that a major shortcoming of the Lambert scattering model is that it does not accurately model darker surfaces. That is one major motivation for developing the Lommel-Seeliger model. However, does this mean that the Lommel-Seeliger model is sufficient to handle bright surfaces? In general, the answer is "no" - the fact that the Lommel-Seeliger model makes the aforementioned assumption that secondary scattering events are ignored means that in cases of dark materials, neglible amounts of light are ignored, but in the cases of brighter surfaces, non-negligible amounts of light are ignored, leading to large inaccuracies.

4.2Lunar Lambert

The Lunar Lambert model is an attempt to handle the Lommel-Seeliger model's inaccuracies in dealing with bright surfaces by combining the Lambert and



Figure 3: The Lunar Lambert Model in which A and B are weighted equally (at .5)

Lommel-Seeliger models. The Lunar Lambert model takes the following form:

$$r = A \frac{\mu_0}{\mu + \mu_0} \cdot B\mu_0$$

Note that the first term has the same form of the Lommel-Seeliger model, while the second term is simply the Lambertian term. The parameters A and B are user parameters that simply reflect how much of which term we wish to weigh. Note that it can also be complex-valued as to model a particle phase function.

The following results of implementing the Lunar Lambert model are as follows:

4.3 Minnaert

The Minnaert model is basically a generalized form of the Lambertian scattering model of the form:

$$r = k\mu_0^n \mu^{n-1}$$

In practice, the Minnaert model has worked on a wide range of objects to model diffuse reflection. However, from a derivation-from-first-principles point of view, there are points on the limbs of the surface in which the reflectance becomes infinite or zero.

Note that by setting n = 1, you have a Lambertian model. The following image depicts the Moon using the Minnaert model.



Figure 4: A figure of the moon depicting the effects of the Minnaert reflection model.

4.4 Hapke

The Hapke model is much more complex than the previous models in that it attempts to correct for the angular distribution of scattering, scattering of light between particles, opposition surge, and the roughness of surfaces. In the following sections, we will briefly discuss these phenomena and their role in diffuse scattering.

4.4.1 Particle Phase Function

The particle phase function of a scattering particle describes in what direction a particle is likely to be scattered. It can be thought of as a radial version of a probability density function. One of the most useful particle phase functions—which has proven to be useful in a variety of situations, is the Henyey-Greenstein phase function, which was first devised by two astronomers examining interstellar radiation. There are multiple variants of the Henyey-Greenstein phase function, including an oft-used two-term formulation, and an even more complex three-term variant. For our purposes, we shall restrict ourselves to the one-term variant:

$$P(\alpha) = \frac{1 - \zeta^2}{(1 + 2\zeta \cos\alpha + \zeta^2)^{3/2}}$$

The ζ parameter essentially determines whether backscattering or forward scattering predominates. In the case that $\zeta=0$, the scattering is isotropic. The closer it is to -1, the more backscattering dominates, and the closer to 1 the ζ parameter is, the more forward scattering dominates.

4.4.2 Multiple Scattering

To correct for multiple-scattering, we introduce the mathematical concept of H-Functions. H-Functions were first introduced by the astronomers Victor Ambartsumian and Subrahmanyan Chandrasekhar, a pair of astronomers who first solved the radiative transfer problem in cases where one wishes to account for multiple scattering. The H-Function in the form given by Ambartsunian and Chandrasekhar cannot be computed analytically, but Hapke gives a simple approximation that is accurate to within a few percent:

$$H(x) = \frac{1 + 2x}{1 + 2x\sqrt{1 - w}}$$

It is worth noting that this approximation makes the isotropic multiple-scattering approximation, or the idea that after multiple bounces light will tend to randomize itself out after multiple bounces; there is no preferential direction to which the light scatters.

4.4.3 Opposition Surge

The Hapke model also includes a term to account for opposition surge, or the illumination of particles when it is backlit from behind. However, we are not particularly concerned with this term since for our purposes, there are often multiple light sources, there are large amounts of ambient light, etc. For the sake of completness we include the formula for opposition surge here:

$$B(\alpha) = \frac{B_0}{1 + (\frac{1}{h}) \cdot \tan \frac{\alpha}{2}}$$

Where α is the angle between the viewer and the light source. It should be noted that the h-term is a measure of the width of the opposition surge. For those interested in implementing this phenomenon, one should consult Hapke [1986] for experimentally determined values.

4.4.4 Surface Roughness

The Hapke model also handles surface roughness with a complex set of equations given in which the four inputs are the roughness parameter θ , the angle between light source and viewer α , and the two parameters i and e, which model the effective angles of incidence and emission. The equations are as follows:

Let:

$$\theta_p = (1 - r_0)\theta$$

$$f(\psi) = \exp(-2tan\frac{\psi}{2})$$

$$\chi(\overline{\theta_p}) = \frac{1}{(1 + \pi tan\theta_p^2)}^{1/2}$$

$$E_1(y) = exp(\frac{-2}{\pi}cot\overline{\theta}_pcoty)$$

$$E_2(y) = exp(-\frac{1}{\pi}cot^2\overline{\theta_p}coty)$$

$$\eta(y) = \chi(\overline{\theta p})[\cos y + \sin y \tan \theta_p \frac{E_2(y)}{2 - E_1(y)}]$$

In the case where e is less than or equal to i:

$$S(i, e, \psi) = \frac{\mu_e}{\eta(e)} \frac{\mu_0}{\eta(i)} \frac{\chi(\overline{\theta_p})}{1 - f(\psi) + f(\psi)\chi(\overline{\theta_p})[\mu/\eta(e)]}$$

$$\mu_{0e} = \chi(\overline{\theta}_p) \left[\cos i + \sin i \cdot \tan \overline{\theta_p} \frac{E(i) - \sin^2(\psi/2) E_2(e)}{2 - E_1(i) - (\psi/\pi) E_1(e)}\right]$$

$$\mu_e = \chi(\overline{\theta}_p)[\cos e + \sin e \cdot \tan\overline{\theta}_p \frac{\cos \psi E_2(i) + \sin^2(\psi/2)E_2(e)}{2 - E_1(i) - (\psi/\pi)E_1(e)}]$$

In the case where i is less than e:

$$S(i,e,\psi) = \frac{\mu_e}{\eta(e)} \frac{\mu_0}{\eta(i)} \frac{\chi(\overline{\theta_p})}{1 - f(\psi) + f(\psi)\chi(\overline{\theta p})[\mu/\eta(i)]}$$

$$\mu_{0e} = \chi(\overline{\theta}_p) \left[\cos i + \sin i \cdot \tan \overline{\theta}_p \frac{\cos \psi E_2(e) + \sin^2(\psi/2) E_2(i)}{2 - E_1(e) - (\psi/\pi) E_1(i)}\right]$$

$$\mu_e = \chi(\overline{\theta}_p) \left[\cos e + \sin e \cdot \tan \overline{\theta}_p \frac{E_2(e) - \sin^2(\psi/2) E_2(i)}{2 - E_1(e) - (\psi/\pi) E_1(i)}\right]$$

4.4.5 Putting it All Together

Combining all these concepts, the final form of the Hapke model is:

$$r = \frac{w}{4\pi} \frac{\mu_{0e}}{\mu_e + \mu_{0e}} \{ P(\alpha)[1 + B(\alpha)] + H(\mu_e)H(\mu_{0e}) - 1 \} S(i, e, \alpha, \overline{\theta})$$

It is worth remembering that because we do not implement coherent backscattering, the Hapke model reduces down to:

$$r = \frac{w}{4\pi} \frac{\mu_{0e}}{\mu_e + \mu_{0e}} \{ P(\alpha) + H(\mu_e) H(\mu_{0e}) - 1 \} S(i, e, \alpha, \overline{\theta})$$

The following image shows the Moon implemented with the Hapke model. Note the distribution of light can be said to be more nuanced, or perhaps even realistic, due to explicitly accounting for the aforementioned several effects.



Figure 5: The Moon lit using the Hapke Reflection Model

5 A Note on Other Models

The four models presented here are only an introduction to the set of BRDFs that are used to model diffuse reflection. A general introduction to those that are commonly used in computer graphics can be found in the 2009 paper by Kurt and Edwards.

In this section, we introduce, and describe the features of some other BRDFs, but we shall not implement them. The interested reader can consult Hapke for the details for implementation.

The semi-empirical Lumme-Bowell model has been adopted by the International Astronomical Union to describe the phase function of asteroids. It is similar to the Hapke function in that the it captures a term for multiple scattering, which it models with H functions. The empirical phase function in the Lumme-Bowell model was made using data from fitting the phase functions of a number of particles measured in the lab by the paper's authors.

The key feature of the Buratti-Veverka model treats depressions in surfaces as paraboloids of revolutions instead of simpler V-shaped grooves, or microfacets. The roughness correction is described by a non-analytic function, so it must be numerically computed on the fly. The model contains several intuitiev adjustable parameters, such a value to control the size and number of the parabolic depressions, as well as parameters to describe the volume-averaged particle phase function. Several solar system bodies, such as the moons Iapetus and Titan, as well as the rings of Saturn have been analyzed using the Buratti-Veverka Model.

The Shkuratov Reflective Model is a complex model that captures both scattering due to coherent backscattering, as well as the shadow-hiding oposition effect. There exists some controversy over whether it is truly accurate, but it has been used with some success in modelling surfaces with large amounts of regolith – such as the moon. Of the three models introduced in this section, it is the most complex, and probably the most difficult to implement (even if all the terms can be analytically evaluated).

References

- [1] Hapke, B. (1986). Bidirectional reflectance spectroscopy. Icarus, 67(2), 264-280. doi: 10.1016/0019-1035(86)90108-9
- [2] Hapke, B. (2012). Theory of reflectance and emittance spectroscopy. Cambridge: Cambridge University Press.
- [3] Shepard, M. (2017). Introduction to planetary photometry (1st ed., p. 263). Cambridge: Cambridge University Press.
- [4] Ray Tracing in One Weekend Series: https://raytracing.github.io/ (Accessed: January 21, 2022)
- [5] Kurt, M., & Edwards, D. (2009). A survey of BRDF models for computer graphics. ACM SIGGRAPH Computer Graphics, 43(2), 1-7. doi: 10.1145/1629216.1629222.
- [6] Lumme, K., & Bowell, E. (1981). Radiative transfer in the surfaces of atmosphereless bodies. I - Theory. II - Interpretation of phase curves. The Astronomical Journal, 86, 1694. doi: 10.1086/113054
- [7] Shkuratov, Y. (1982) A model for negative polarization of light by cosmic bodies without atmospheres. Sov. Astron., 26, 493–6.
- [8] Buratti, B., & Veverka, J. (1985). Photometry of rough planetary surfaces: The role of multiple scattering. Icarus, 64(2), 320-328. doi: 10.1016/0019-1035(85)90094-6